



HAL
open science

Routing in mobile aerial networks

Violet R. Syrotiuk, Charles J. Colbourn

► **To cite this version:**

Violet R. Syrotiuk, Charles J. Colbourn. Routing in mobile aerial networks. WiOpt'03: Modeling and Optimization in Mobile, Ad Hoc and Wireless Networks, Mar 2003, Sophia Antipolis, France. 9 p. inria-00466673

HAL Id: inria-00466673

<https://inria.hal.science/inria-00466673>

Submitted on 24 Mar 2010

HAL is a multi-disciplinary open access archive for the deposit and dissemination of scientific research documents, whether they are published or not. The documents may come from teaching and research institutions in France or abroad, or from public or private research centers.

L'archive ouverte pluridisciplinaire **HAL**, est destinée au dépôt et à la diffusion de documents scientifiques de niveau recherche, publiés ou non, émanant des établissements d'enseignement et de recherche français ou étrangers, des laboratoires publics ou privés.

Routing in Mobile Aerial Networks

Violet R. Syrotiuk Charles J. Colbourn

Department of Computer Science & Engineering
Arizona State University
P.O. Box 875406
Tempe, AZ 85287-5406
e-mail: {syrotiuk,colbourn}@asu.edu

Abstract

The problem of routing in unmanned aerial vehicles (UAVs) flying circular flight patterns equipped with directional antennas is considered. The active communication links are modelled as trigonometric functions of time. As a result, transmission opportunities can be computed on demand, resulting in a simple distributed routing protocol. Each UAV has a very compact representation (using only five parameters), and so the model is particularly advantageous in aerial networks where the vehicles may be dynamically redeployed to a different air space. Results from numerical solution of the equations using Maple mathematical software are presented, to show surprising complexity in the windows of transmission opportunities.

1 Introduction

The battlefield of the future is planned as a hierarchical ad hoc network with airborne, ground, and soldier forces. One such plan is the U.S. DARPA/Army Future Combat Systems program [2], which includes the emergence of unmanned platforms as a viable alternative to manned platforms. The interest in unmanned platforms has been renewed in recent years by better technology to support wide area data links at video data rates, as well as smaller, more powerful computers that allow more reliable autonomous operation. In turn, these technological advances permit increased flexibility in the missions planned. Another factor driving the interest in unmanned platforms includes a political climate that demands no loss of personnel. This demand may be best achieved when the missions are too dangerous or too repetitive to be delegated to manned vehicles.

In the air, *unmanned aerial vehicles* (UAVs) are

used for the purposes of intelligence, surveillance, and reconnaissance. While there are many tactical applications of UAVs, there are also peace-time applications [1]. For example, a UAV can provide information on the number of people displaced or survey damage in the event of severe weather. Such information can be useful in support of humanitarian aid missions. UAVs have also been used to monitor compliance with United Nations resolutions. As well, drug enforcement blockade and quarantine missions may be supported by UAVs. This frees the enforcement patrol assets for other duties.

The variety of UAVs ranges greatly in size and capability (see [17] for a good overview). Our interest is in the endurance category of UAV. One example in this category is the Global Hawk [3], an aircraft that can range as far as 12000 nautical miles, at altitudes up to 65000 feet (20000 meters), flying at speeds approaching 340 knots (about 400 mph) for as long as 35 hours. During a typical mission, the aircraft can fly 1200 miles to an area of interest and remain in a flight pattern for 24 hours.

Typically, UAVs are equipped with sensors for detecting emissions (e.g., RF, acoustic, magnetic, meteorological, thermal, multi-spectral) as well as foliage penetration. Through the UAVs, these emissions may be relayed air-to-air and then air-to-ground in near real-time. This reduces delay and preserves the energy of the ground forces, since the communications equipment in the UAVs has a larger transmission radius and is not as resource constrained.

In this paper, we focus on the airborne forces of a future battlefield and examine the problem of routing between the UAVs. As Figure 1 shows, we consider a number of UAVs, each equipped with a directional antenna, flying in a circular flight pattern. In our model, we represent the active communication links by trigonometric functions of time. Rather than pro-

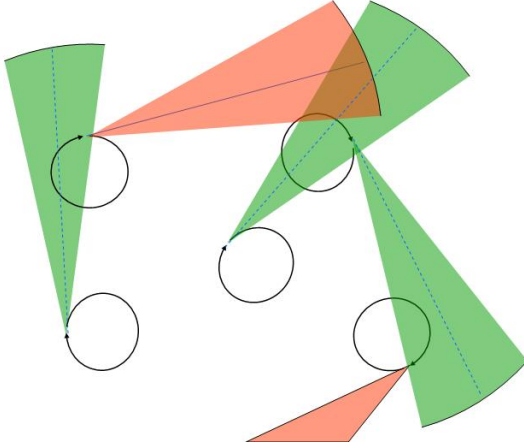


Figure 1: Sample aircraft geometry.

duce an explicit schedule for each link, we represent it implicitly in the form of these trigonometric functions and solve them only when they are actually needed. Routing is then accomplished in a distributed manner by computing, upon request, the next time that a link is available. This in turn can be used in a dynamic Dijkstra's algorithm to compute shortest paths. The advantage of this representation is that it allows for flexibility in case of redeployment or reassignment of the UAVs to a different air space since only five parameters for each vehicle is needed: the center of the flight pattern, flight radius, orientation, initial position, and speed.

The rest of this paper is organized as follows. In Section 2 we introduce our model of mobile aerial networks through the use of trigonometric functions of time (more precisely, rational polynomials of trigonometric functions). Since the network may be viewed as a graph whose edges appear and disappear over time, we place our model in context of other models for dynamically evolving graphs. Section 3 shows examples of transmission opportunities in some sample scenarios solved numerically using Maple [14]. The complexity in the windows of transmission opportunity is rather surprising, indicating that the period of the graph sequence may be very long. Section 4 gives the routing protocol, essentially a modification of Dijkstra's algorithm, and describes a variation that anticipates link existence to reduce delay. Finally, we propose extensions of this work and conclude in Section 5.

2 Modelling Aerial Networks

We model a mobile aerial network with n unmanned aerial vehicles. Each UAV U_i , $0 \leq i < n$, is specified by five parameters that describe its flight pattern (see Figure 2):

1. The point (a_i, b_i) is the center of the circular flight pattern.
2. r_i is the radius of the flight pattern.
3. The angle $\theta_i(0)$ is the initial angle in radians from the center of the circle when the flight pattern starts.
4. The direction δ_i of flight, which is either clockwise ($\delta_i = 1$) or counter-clockwise ($\delta_i = -1$).
5. The speed s_i at which the UAV is flying. We assume that s_i is constant while a UAV is in its flight pattern.

For simplicity, we initially consider the two-dimensional problem, i.e., all UAVs are flying in the same (geometric) plane.

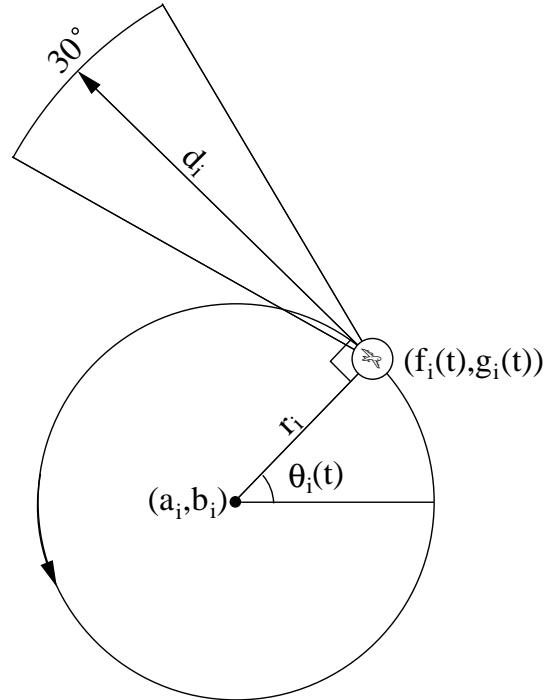


Figure 2: Parameters of UAV configuration.

In general, the position $(f_i(t), g_i(t))$ of U_i is a function of time t and can be expressed as a function of its reference angle $\theta_i(t)$, which is also a function of

time. That is,

$$\begin{aligned} f_i(t) &= a_i + r_i \cos \theta_i(t) \text{ and,} \\ g_i(t) &= b_i + r_i \sin \theta_i(t). \end{aligned}$$

The reference angle $\theta_i(t)$ depends on how far the UAV has travelled in time relative to its initial value,

$$\theta_i(t) = \theta_i(0) + \frac{\delta_i s_i t \bmod 2\pi r_i}{r_i},$$

where mod is a function that reduces into the interval $[0, 2\pi r_i)$.

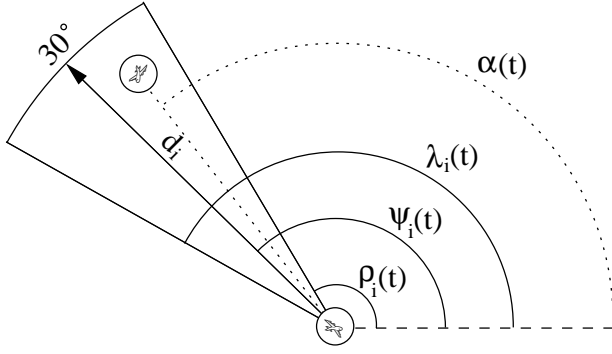


Figure 3: Heading angle, angle and distance trap.

As Figure 3 shows, the UAV flies along the tangent of the circle representing its flight pattern. The direction it is heading $\psi_i(t)$ is always ninety degrees ($\pi/2$ radians) more than the reference angle, i.e.,

$$\psi_i(t) = (\theta_i(t) + \delta_i \cdot \pi/2) \bmod 2\pi.$$

The nose of each UAV is equipped with a directional antenna with a beam width of thirty degrees that is used for transmission. The transmission range d_i , i.e., the beam length of the antenna at the bore-sight, depends on the path loss model. Together, the beam width and length define the transmission cone of U_i . Since the beam width is thirty degrees, the left edge $\lambda_i(t)$ of the cone is fifteen degrees ($\pi/12$ radians) more than the heading angle, while the right edge $\rho_i(t)$ is fifteen degrees less, i.e.,

$$\begin{aligned} \lambda_i(t) &= \psi_i(t) + \pi/12 \text{ and,} \\ \rho_i(t) &= \psi_i(t) - \pi/12. \end{aligned}$$

We assume that omnidirectional mode is used for reception. The position of UAV U_j , $j \neq i$, is also a trigonometric function of time. UAV U_j can receive from UAV U_i if the position of U_j at time t is within the transmission cone of U_i at time t . One way for U_j to look at being “trapped” within the cone is to

simultaneously satisfy a distance trap and an angle trap.

The *distance trap* is satisfied if U_j at position $(f_j(t), g_j(t))$ is within the circle defined by center $(f_i(t), g_i(t))$ and radius d_i . This is true if

$$((f_j(t) - f_i(t))^2 + (g_j(t) - g_i(t))^2) \leq d_i^2,$$

using the standard formula for distance between two points.

The *angle trap* requires that the angle $\alpha(t)$ to U_j relative to the x -axis of U_i at time t , lie between the left and right edges of the transmission cone, i.e.,

$$\rho_i(t) \leq \alpha(t) \leq \lambda_i(t).$$

A transmission opportunity from U_i to U_j exists at time t when both the distance trap and the angle trap are satisfied.

Alternatively, we may solve for t and find the next time that the distance and angle traps are satisfied for a given pair of UAVs.

2.1 Implicit Graph Model

While we defined the transmission cone as a trigonometric function of time, there is an implicit graph structure underlying the model.

The sequence of transmission opportunities can be modelled by a sequence of directed graphs, $\mathcal{G} = G_{t_0} G_{t_1} \dots G_{t_{p-1}}$ over some time horizon p . Here, where the vertex set $V_{t_k} = \{U_0, \dots, U_{n-1}\}, \forall k$. There is an edge $(U_i, U_j) \in E_{t_k}$ from UAV U_i to UAV U_j if the position of U_j at time t_k is within the transmission cone of U_i at time t_k . The next graph in the sequence occurs when an existing edge (U_i, U_j) drops out of the graph, i.e., the position of U_j is no longer in the transmission cone of U_i , and/or when a new edge (U_ℓ, U_m) is added to the graph, i.e., the position of U_m enters the transmission cone of U_ℓ . Similar models for graphs in dynamic scenarios have been defined [9, 4, 12, 13].

As above, we may solve for t (numerically or analytically) and determine the times of transmission opportunities between a pair of UAVs. Assuming that the flight patterns are specified by rational input, the graph sequence is periodic with some period p . That is, at time $t' = (t \bmod p)$ the topology of the network is given by $G_{t'}$. The period of the graph sequence may be quite complex (as seen by the results in Section 3), as *both* endpoints (UAVs) of the edges are in motion. Our approach does not require any knowledge of the period, or even require that the sequence be periodic.

3 Numerical Results on Transmission Opportunities

Figure 4 shows the scenario from which the results in this section were generated. The scenario consists of ten UAVs. Solid circles represent a counter-clockwise orientation whereas dotted circles represent a clockwise orientation.

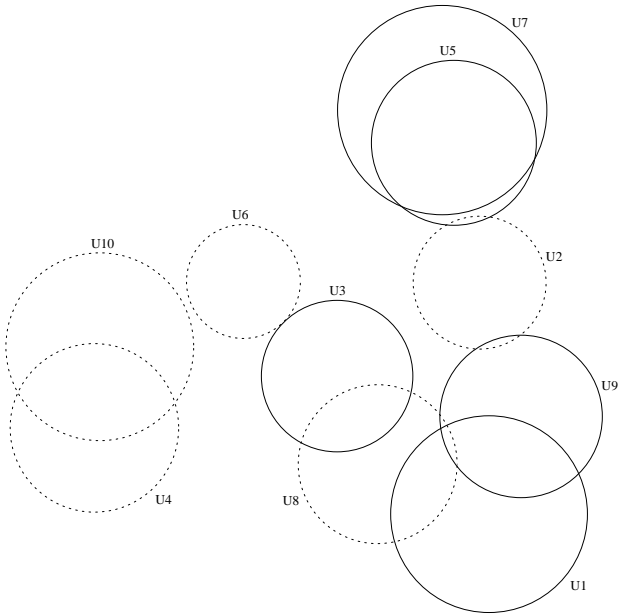


Figure 4: UAV scenario.

Figures 5–15 show a collection of results from this scenario computed using Maple [14], a mathematical software package. We present a number of results in order to illustrate the wide diversity of outcomes obtained.

Each figure is for a destination UAV U_j from the perspective of a source UAV U_i , and is made up of three subfigures each of which is a function of time. The left subfigure illustrates the angle trap. The narrow stripes represent the lines that define the transmission cone of U_i . The closer the stripes, the faster the UAV U_i flies through the circle that is its flight pattern. The angle of the stripes (left/right) indicates the orientation of flight (clockwise/counter-clockwise).

We plot the angle $\alpha(t)$ of U_j from the perspective of U_i as it changes as both UAVs fly through their flight pattern over time. There is an underlying universal frame of reference that all the planes share. When the function falls between the narrow stripes, U_j is within the transmission cone of U_i , i.e., the angle trap is satisfied.

The middle subfigure illustrates the distance trap. The horizontal line indicates the transmission radius, d_i , of U_i . Here, we plot the distance between U_i and U_j as a function of time. If the function is below the line, the distance trap is satisfied. Otherwise, U_j is not in the transmission range of U_i . We have deliberately left our measure of distance and time unitless.

The right subfigure is an indicator function. When the function equals one there are two possible outcomes. If the colour is light then it indicates that the distance trap passed but the angle trap failed. If the colour is black, then the angle trap passed but the distance trap failed. If the function equals two, then both the distance trap and the angle trap passed and U_j may receive a transmission from U_i . White indicates that both tests failed. Currently, this assumes that the transmission delay is negligible. This could be strengthened by taking into account the width of the transmission window, and also by anticipating (computing) when the transmission window is open and having the transmission arrive on the leading edge.

Figures 5–8 show interactions that seem more natural. In these figures, both UAVs are flying in the same orientation. In Figures 5 and 6 while the distance trap is satisfied more than half of the time, the angle trap is rarely satisfied resulting in narrow windows of transmission opportunity. The stripes in the angle trap of Figure 7 indicate that U_8 takes longer to fly through one revolution than U_6 . As a result, the angle traps are wider than in the previous two figures. In this case, U_2 is caught in the angle trap for some time before it then comes into range of U_3 . In Figure 8, both the distance and angle trap windows are quite narrow, yet there are still several transmission opportunities.

In the remaining figures, Figures 11–15, the results become increasingly more unexpected. In Figure 11 the distance trap and angle trap are rarely in synch, resulting in only one transmission opportunity. In Figure 10, the UAVs are rarely close enough for U_7 to transmit to U_3 and when they are, the angle trap is not satisfied. Hence over this time interval, there is not transmission opportunities.

In the case of Figure 11, U_7 is flying clockwise and U_2 is flying counter-clockwise. There is a time near $t = 180$ when U_2 is flying directly into the transmission cone of U_7 and the transmission window opens for a long period of time.

As Figure 12, U_{10} is always within the transmission range of U_4 . As well, the angle trap is often satisfied. This configuration seems to offer the best transmission opportunities.

Figures 13 and 14 are rather unusual since we might expect to catch a UAV in our angle trap once as we travel through one revolution of our flight path. Figure 13 shows that, in one revolution of U_2 's flight pattern, UAV U_9 has three transmission opportunities. This occurs as the two vehicles approach each other. Figure 14 shows that while between U_5 and U_7 the distance trap is occasionally satisfied, the angle trap is not satisfied. In this case, one UAV is essentially in the shadow of the other, i.e., in a “blind spot” where it is never reachable.

In Figure 15 the UAVs are virtually always in transmission range yet the transmission opportunities are quite limited.

In summary, the complex behaviour of the transmission opportunities underlies the requirement to devise a compact representation of the network, i.e., the parameters of each UAV and the functions relating them, in order to be able to compute links and therefore routes on the fly.

4 Routing in Aerial Networks

The optimization problem motivating the search for transmission opportunities is that of finding shortest air-to-air paths between UAVs. The idea is that the emissions collected by the sensors of the UAV may be relayed in a store-and-forward manner to the UAV that best serves a given ground station.

A modified version of Dijkstra’s shortest path algorithm [6] is used. This approach is similar to the scenario of Halpern et al. [11] in which a network of railways with moving trains is considered. There, the track can only be used for travel in one direction, and cannot be used by another train at the same time. Ekici et al. [8] examine the problem of routing in low earth orbit satellites. In this configuration, the satellites always have the same neighbours which are closer at higher latitudes, and transmission is not allowed over the polar regions.

The graph is obtained by determining the pairs for which a connection exists at some point in time. The essential modification of Dijkstra’s algorithm lies in the calculation of edge lengths dynamically.

Suppose that, at some stage of Dijkstra’s algorithm, the vertex w is entering the set of vertices to which the shortest path is known with certainty, and suppose that the distance to w is t_w . Then for every vertex x which is a successor of w , we must determine the time t_x so that $t_x \geq t_w$, edge (w, x) exists at time t_x , and t_x is as small as possible subject to these constraints. Having computed t_x in this manner, we check whether this value is lower than the

previously computed shortest path estimate for x . If it is, we use t_x as the new shortest path estimate for x .

Thus the “length” of an edge depends essentially upon the time at which one tries to communicate along the edge; but the length can be computed at the time that the edge may be useful. Since this calculation can be done only once for each edge, it does not impact the run time analysis given in [10, 16].

This solution does not account for any queueing delays incurred at intermediate nodes. As well, as we have already mentioned, it assumes that transmissions are essentially instantaneous.

5 Summary and Future Work

In this paper, we have considered the problem of routing in mobile aerial networks. Trigonometric functions are used to represent the window of transmission opportunity between UAVs since the transmitters are directional. These in turn can be used to determine (or predict) link existence, thereby allowing a simple distributed routing protocol to be used (based on Dijkstra’s algorithm). A surprising variation in transmission opportunities was found.

We used Maple [14] to obtain our results numerically. We are now interested in the continuous optimization of the trigonometric functions by approximation with exponential or logarithmic functions.

Our current model makes many simplifying assumptions. Some ways in which the model may be extended is to include physical transmission effects which may require retransmissions in the event of transmission errors, transmission delay, and the ability to buffer at the UAVs. Other extensions to improve realism include considering the problem in three dimensions and incorporating terrain models, such as those used in modSAF [15].

Currently, the flight patterns of the UAVs are assumed to be circular. They could instead be elliptical or figure-8, for example. As well, not all UAVs need to follow the same type of flight pattern. Nevertheless, the destination is assumed not to change flight patterns to enhance or reduce the time required to complete message delivery, as in “moving target search” [5, 7].

In conclusion, the problem of routing in mobile aerial networks has work has raised many questions whose solution is required to support heterogeneous ad hoc networks of the future.

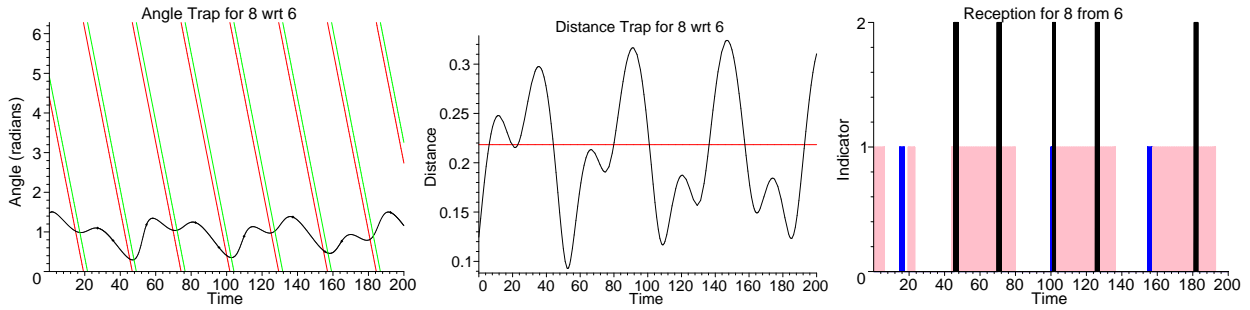


Figure 5: U_6 has several transmission opportunities to U_8 .

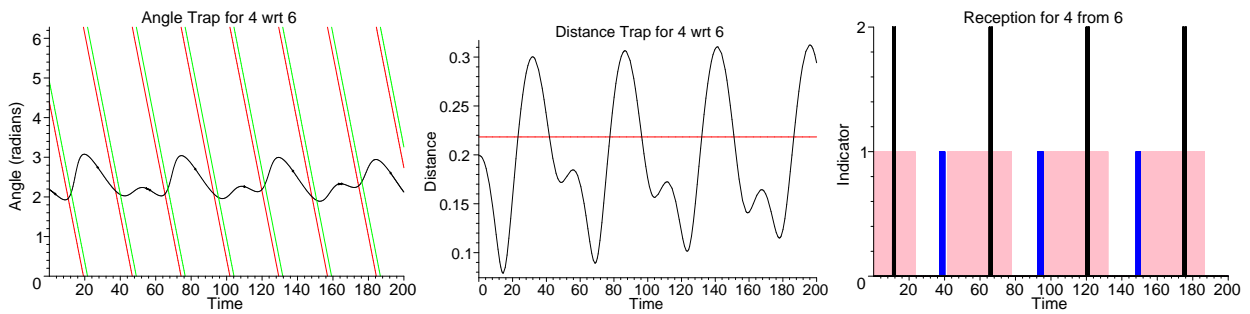


Figure 6: Angle trap approaching distance trap at head of distance window.

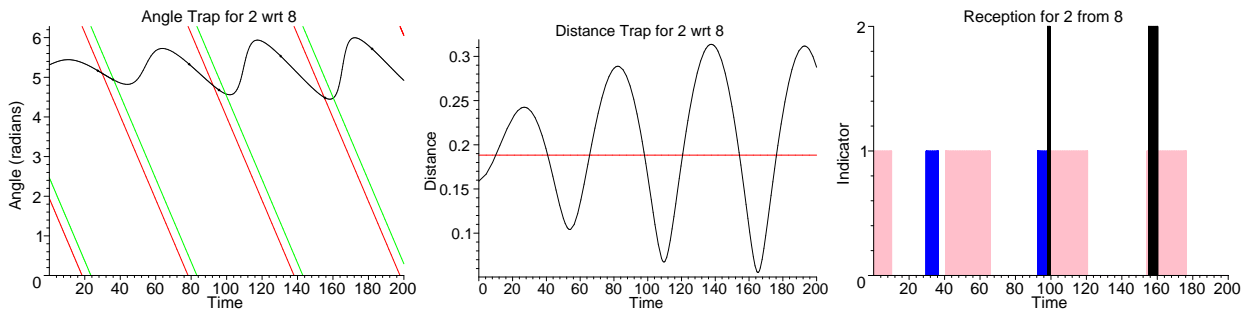


Figure 7: Angle trap satisfied first, then both conditions, and angle is lost.

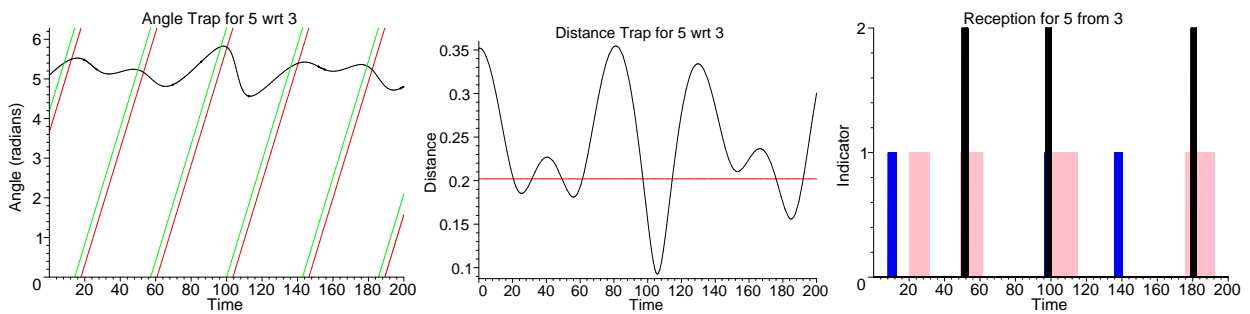


Figure 8: Shorter distance traps, yet many transmission opportunities.

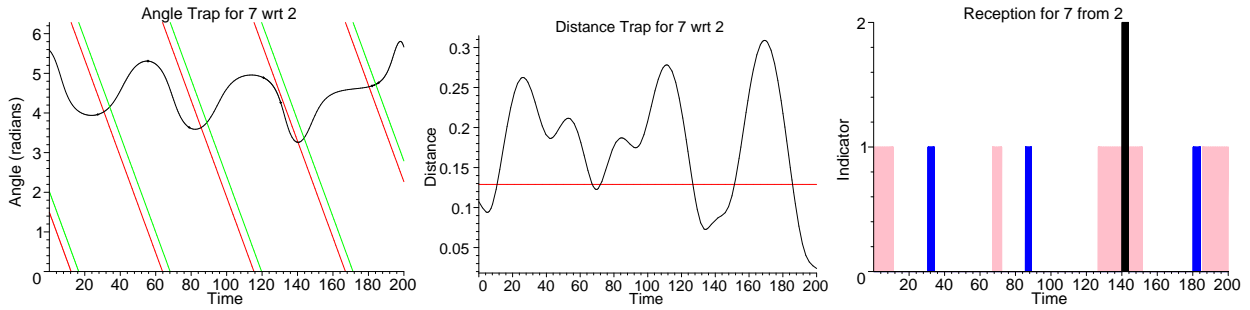


Figure 9: Fewer transmission opportunities in the short distance traps.

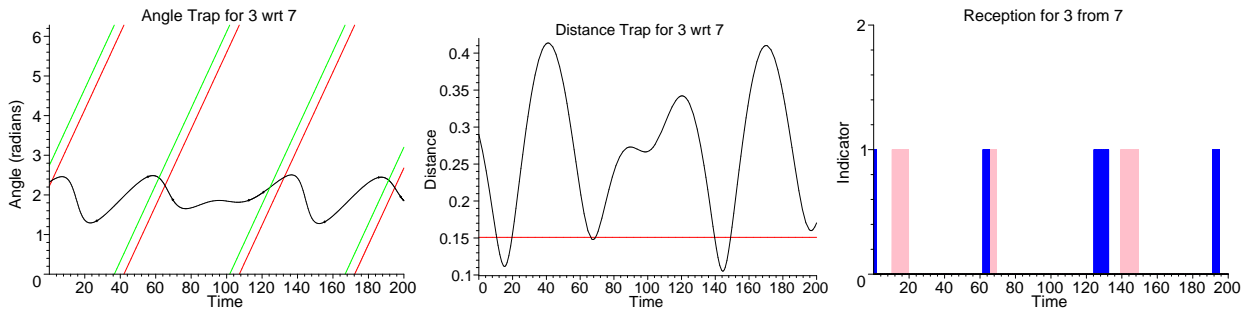


Figure 10: The angle and distance trap are never simultaneously satisfied over this time period.

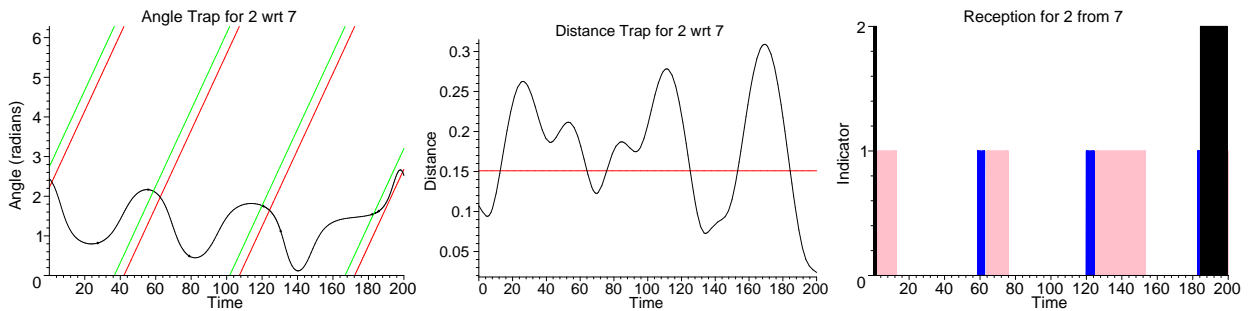


Figure 11: Large transmission window when U_2 flies into U_7 's transmission cone.

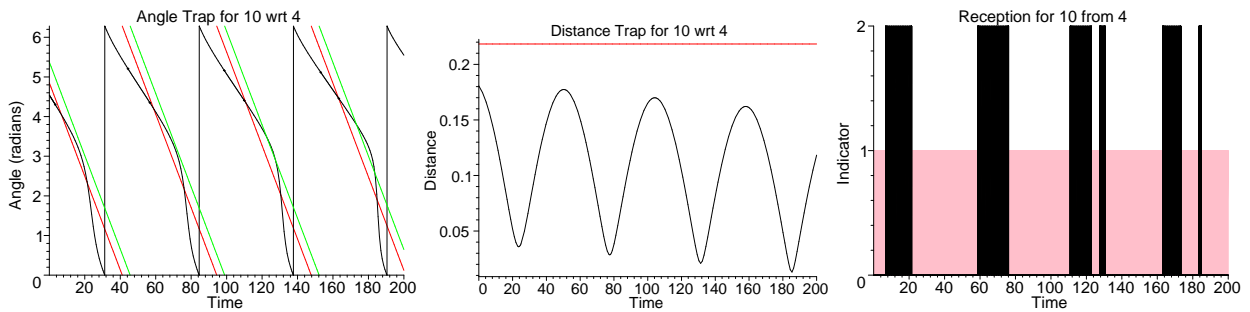


Figure 12: U_{10} is always in range of U_4 ; broad transmission windows.

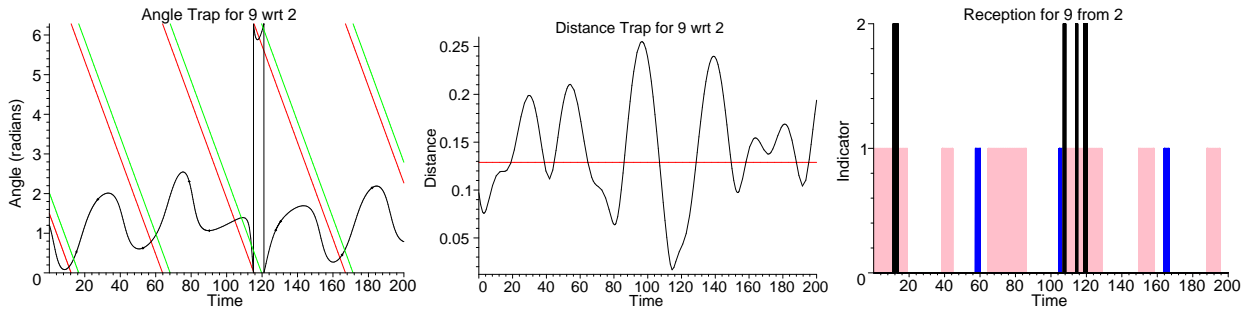


Figure 13: Example showing U_9 “seen” by U_2 three times in one circle of its flight pattern.

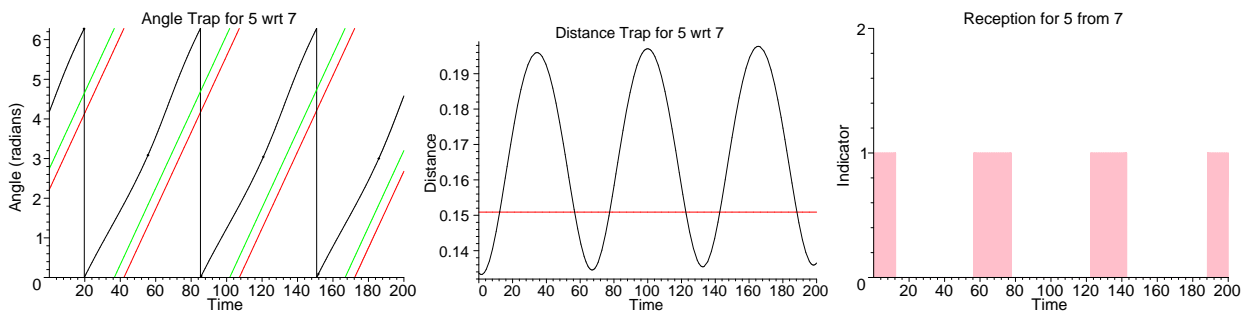


Figure 14: Example of a “blind spot;” U_7 never “sees” U_5 even though the distance trap may be satisfied.

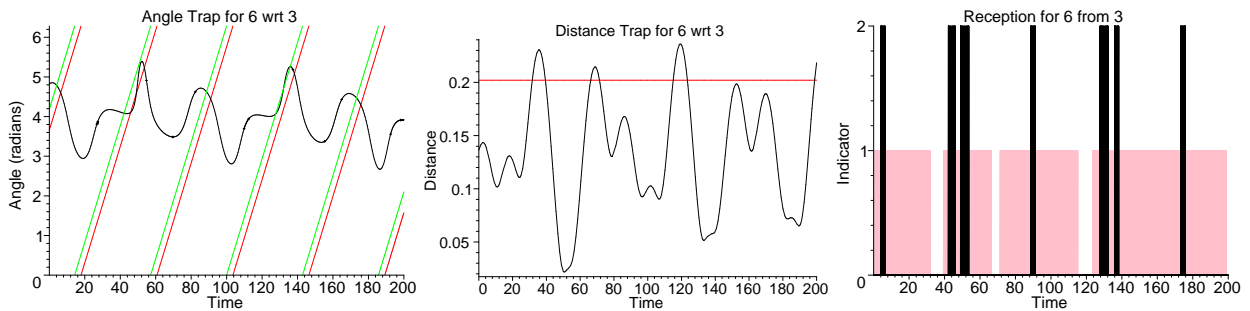


Figure 15: U_6 almost always is in the distance trap, yet few transmission opportunities.

Acknowledgment

We are grateful to John Powers, Bob Flanagan, and Bruce Munro of Raytheon Company in Plano, Texas for providing the motivation for this research.

References

- [1] Air Combat Command, “Concept of Operations for Endurance Unmanned Aerial Vehicles,” December 1996.
http://www.fas.org/irp/doddir/usaf/conops_uav/index.html
- [2] Defense Advanced Research Projects Agency (DARPA), Future Combat Systems (FCS).
<http://www.darpa.mil/fcs/index.html>
- [3] Aeronautical Systems Center, U.S. Air Force Fact Sheet, Global Hawk.
<http://www.af.mil/news/factsheets/global.html>
- [4] S. Bhadra and A. Ferreira, “Computing Multicast Trees in Dynamic Networks using Evolving Graphs,” Institut National de Recherche en Informatique et Automatique (INRIA), Research Report No. 4531, August 2002, revised October 2002.
- [5] F. Chimura and M. Tokoro, “The Trailblazer Search: A New Method for Searching and Capturing Moving Targets,” *Proceedings of the Twelfth National Conference on Artificial Intelligence* (Menlo Park, CA), 1994, pp. 1347–1352.
- [6] E.W. Dijkstra, “A Note on Two Problems in Connexion with Graphs,” *Numerische Mathematik* 1 (1959), pp. 269–271.
- [7] S. Edelkamp, “Updating Shortest Paths,” *Proceedings of the European Conference on Artificial Intelligence (ECAI)* (Brighton, UK), 1998, pp. 655–659.
- [8] E. Ekici, I.F. Akyildiz, M.D. Bender, “A Distributed Routing Algorithm for Datagram Traffic in LEO Satellite Networks,” *IEEE/ACM Transactions on Networking* (April 2001), Vol. 9, No. 2, pp. 137–147.
- [9] A. Faragó and V.R. Syrotiuk, “MERIT: A Unified Framework for Routing Protocol Assessment in Mobile Ad Hoc Networks,” *Proceedings of the Seventh Annual International ACM Conference on Mobile Computing and Networking (Mobi-com’01)*, (Rome, Italy), July 2001, pp. 53–60.
- [10] M.L. Fredman and R.E. Tarjan, “Fibonacci Heaps and their Uses in Improved Network Optimization Algorithms,” *Journal of the ACM* 34 (1987), pp. 596–615.
- [11] J. Halpern and I. Priess, “Shortest Path with Time Constraints on Movement and Parking,” *Networks*, 4, 1974, pp. 241–253.
- [12] P. Haxell, A. Rasala, G. Wilfong, and P. Winkler, “Wide-Sense Nonblocking WDM Cross-Connects,” *Proceedings of the Tenth European Symposium on Algorithms (ESA) 2002*, LNCS 2461, pp. 538–550.
- [13] E. Köhler, K. Langkau, and M. Skutella, “Time-Expanded Graphs for Flow-Dependent Transit Times,” *Proceedings of the Tenth European Symposium on Algorithms (ESA) 2002*, LNCS 2461, pp. 599–611.
- [14] Maple 8, Waterloo Maple, Inc.
<http://www.maplesoft.com/main.html>
- [15] ModSAF, Modular Semi-Automated Forces.
<http://www.ait.nrl.navy.mil/modsaf/modsaf.html>
- [16] K. Noshita, “A Theorem on the Expected Complexity of Dijkstra’s Shortest Path Algorithm,” *Journal of Algorithms* 6 (1985), pp. 400–408.
- [17] UAV Forum.
<http://www.uavforum.com>